# Fully automated system for simultaneous measurement of thermal conductivity and heat capacity from 4 to 300 K

R. S. Kwok

*Department of Physics and Solid State Science Center, University of California, Los Angeles, California 90024*

S. E. Brown

*Physics Division, Los Alamos National Laboratory, Los Alamos, New Mexico 87545*

(Received 31 July 1989; accepted for publication 16 October 1989)

A fully automated system which is capable of measuring specific heat and thermal conductivity simultaneously from liquid helium to room temperature is presented. Thermal conductivity is measured by a steady-state longitudinal heat flow technique, and specific heat by a thermal relaxation method. A numerical simulation of the one-dimensional heat flow equation is used to examine the basic operational principle. The method is tested using GE 214 fused quartz and AISI 304 stainless-steel rods, and the results compare favorably with values quoted in the literature.

## INTRODUCTION

Thermal conductivity and heat capacity are two important physical quantities for understanding the physics of solids at various temperatures and for designing cryogenic apparatus. The former quantity reveals the basic heat transport mechanism and the latter is a thermodynamic variable which is of fundamental interest. Measuring these properties simultaneously is useful to eliminate artifacts associated with different samples and/or environments. However, existing systems for simultaneous measurement of both quantities are usually operated either at low temperature[1] or above room temperature.[2] The following is a description of an experimental setup for such a measurement between 4 and 300 K.

## I. PRINCIPLE OF OPERATION

In the absence of convection or radiation, the diffusive, steady-state, unidirectional heat flow through an isotropic medium is given by the Fourier–Biot equation:

$$\dot{Q} = \kappa A \left(\frac{\partial T}{\partial x}\right), \tag{1}$$

where $\dot{Q}$ is the rate of heat flow through an area $A$, with a temperature gradient $\partial T/\partial x$ perpendicular to $A$. The proportionality constant $\kappa$ is the thermal conductivity, and the minus sign indicates that the direction of heat flow is opposite to the temperature gradient.

If the temperature of the specimen varies with time at a rate $\dot{T}$, and the thermal conductivity is independent of the temperature change, one can derive from the continuity principle that

$$\dot{T} = D\frac{\partial^2 T}{\partial x^2}, \tag{2}$$

where $D = \kappa/\rho C$ is the thermal diffusivity, $\rho$ is the mass density, and $C$ is the specific heat of the specimen in J/gm K.

Measurements of $\kappa$ are usually characterized as "static" (or steady state) if they are made on a specimen with a time-independent temperature distribution and satisfy Eq. (1), or as "dynamic" (or transient) if the specimen temperature varies with time during the measurement and follows Eq. (2). The latter usually yields values of thermal diffusivity rather than of $\kappa$ directly. Thus, one can measure $\kappa$ with a static method and then determine values of $C$ by measuring the diffusivity with a dynamic method. This is the basic concept of our design.

One of the most common transient methods for measuring $C$ is often referred to as the thermal relaxation method.[4] In this method, a sample at temperature $T$ connects with a heat reservoir at a temperature $T_0 < T$ through a weak heat link of thermal conductance $K$. The temperature of the sample, after switching off the attached heater, is given by

$$c\dot{\theta} = -K\theta, \tag{3}$$

where $\theta \equiv (T - T_0)$ and $c$ is the heat capacity of the specimen. Equation (3) implies that a discontinuous change in $\dot{Q}$ from one constant value to another will be followed by an exponential approach to the steady state, i.e.,

$$\theta(t) = \theta(0)\exp(-t/\tau), \tag{4}$$

where $\tau = c/K$ is the time constant (often called the thermal relaxation time) and is inversely proportional to the thermal diffusivity such that $\tau = L^2/D$ with $L$ the sample length.

We employ the same relaxation method for measurement of $C$, with the difference that the heat link is the sample itself. To ensure that Eq. (4) is valid for our setup, we have investigated the temperature profile of the specimen by a computer simulation. Details of the study will be discussed in Sec. III.

## II. APPARATUS

### A. Experimental setup

Thermal conductivity measurements reported in the TPRC[5] data books are most commonly performed with a steady-state linear heat flow method, even though different apparatuses give slightly different results depending on the

 0034-6748/90/020809-05$02.00  

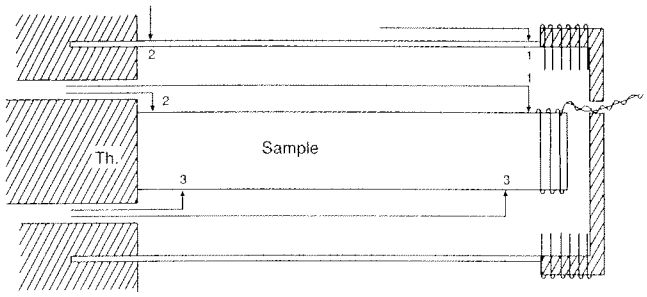


FIG. 1. Schematic diagram of the sample chamber. 1, 2, and 3 are the 3 pairs of thermocouples TC1, TC2, and TC3 discussed in text. Th. is the location of two thermometers. Shaded parts are made of copper. The shield is adjustable in length and is made of stainless steel.

details of the experiment. Our design, based on the same principle in which Eq. (1) applied, is shown in Fig. 1. The specimen under study, typically with a diameter of 1–2 mm and length of 1–2 cm, is attached to the copper thermal reservoir by a thermally conductive epoxy Thermalbond[6] 4951. The other end of the specimen is wrapped with a resistive wire heater and the power dissipated is determined by measuring the voltage across and current through the heater. A stainless steel radiation shield (thickness 0.4 mm), with adjustable length and a diameter approximately 2–4 times that of the sample, is clamped onto the copper base to ensure good thermal contact. The other end of the shield is soldered to a copper piece on which a heater wire is wrapped. This arrangement provides an uniform temperature region at the heater end of the sample to minimize radiation loss from the sample heater. A carbon-glass (CGR) and a platinum resistor (PTR) are embedded in the copper block (marked as Th. in Fig. 1) to determine the base temperature.

Three pairs of differential thermocouples (TC) which attach to the shield and the specimen, are connected at the outer end of the base so that heat conduction through the TC is minimized. The first thermocouple (TC1 in Fig. 1), which connects the shield and the specimen at the hot end, is used to control the shield temperature such that TC1 should register zero voltage during the whole experiment. The second TC, which connects the shield and the specimen at the base end, is used to monitor the boundary thermal resistance between the sample and the base. The voltage across TC2 should remain small throughout the experiment. The third, TC3, is used to measure the temperature difference between two points on the sample.

The cell shown in Fig.1 is enclosed by a copper can on which a uniformly spaced heater wire is wrapped. The can is used as an additional radiation shield as well as the main heat source to maintain a constant base temperature.

By matching the temperature profile of the shield to that of the sample, the radiation heat loss along the sample is minimized. Consequently, all the power input through the sample heater flows longitudinally along the specimen. The entire experiment is operated under vacuum so there is no convective heat loss as well. Therefore, Eq. (1) is valid for our $\kappa$ measurement. By switching off both the sample and shield heaters, we observe an exponential temperature decay obeying Eq. (4) from which $\tau$ and $C$ can be determined.

## B. Electronics

Signals from the thermocouples are registered by either a Keithley 181 nanovoltmeter or a Keithley 150B microvoltmeter. The voltage from TC1 also feeds back into a home-built[7] temperature controller which is used to match the temperature of the shield to that of the sample at the hot end. A Quantum Design 1802 digital R/G bridge is used as the base temperature controller as well as a constant current source for the sample heater. The exponential decay of $\Delta T$ is recorded by a Hewlett-Packard 3457A multimeter which is capable of reading a series of signals as close as 2 ms after switching off the heaters and 20 ms between readings. The time delays between readings are constantly adjusted by the computer so that 300 data points are recorded between $t \simeq 0$ and $1.2\tau$ for each decay curve.

## C. Principle of automation

The system is fully controlled by an IBM personal computer during the entire experiment. All controlling parameters are preset by the computer but can be changed anytime by the operator. Computer codes used for the measurement are divided into steps as shown in Fig. 2.

The system usually takes about 15–60 min to reach steady state depending on the temperature increment between data points and the relaxation time constant of the specimen. Another 5–20 min is normally sufficient for actual data recording so that the standard deviation of $\kappa$ is $< 0.5\%$. In order to get a smooth decay curve of $\Delta T$ for the diffusivity measurement, the procedures are repeated several times and the sum of the signals is then averaged. By doing so, the uncertainty in $\tau$ evaluated is usually $< 2\%$.

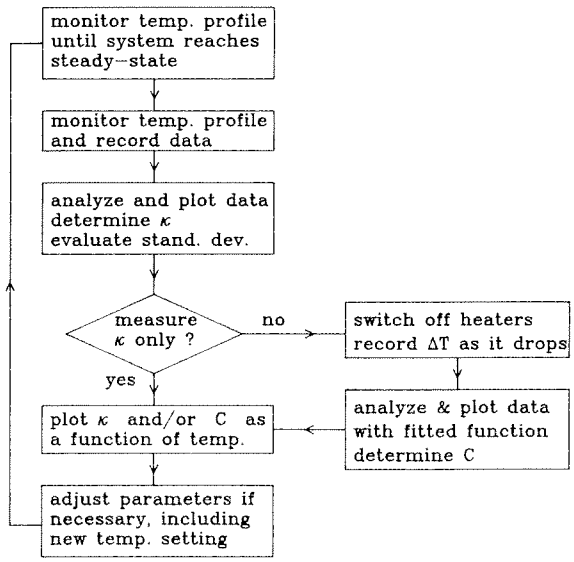


FIG. 2. Flow chart of the algorithm for entire experimental procedure.

## III. NUMERICAL TEST

The temperature distribution $T(x,t)$ of the sample is dictated by the heat flow equation [Eq.(2)]. Knowing the exact temperature profile at $t = 0$, one can in principle solve for $T(x,t)$ at any time $t > 0$. In our case, the initial conditions can be approximated by

$$T(0,t) = T(0,0)$$

and

$$T(x,0) = T(0,0) + P_0 x/KL \quad \text{for} \quad 0 \leqslant x \leqslant L,$$

where $x = 0$ is defined as the end of the sample connected to the base, and $P_0$ is the constant power input through the heater wire at $t = 0$ as described earlier.

Under the ideal operating conditions, the temperature of the heater end of the sample ($x = L$) is the same as that of the shield ($x > L$), so that there is no radiation heat loss. One can therefore assume that $\partial T/\partial x = 0$ for $x > L$.

Solving this problem analytically is nontrivial due to the singularity of $\partial T/\partial x$ at $x = L$. Nevertheless, it is clear from the above equations that $\partial^2 T/\partial x^2 < 0$ at $x = L$ and therefore initiates the temperature drop at $x \simeq L$ for any finite $t > 0$. The rest of the sample (especially for $x \ll L$) remains at a constant temperature for $t \ll \tau$ because of the constant $\partial T/\partial x$ at $t = 0$.

To study $T(x,t)$ of the sample quantitatively, we constructed the following one-dimensional model. Suppose the specimen can be divided into $N$ equal segments and that the conservation of energy gives

$$K_i(T_{i+1} - T_i) = c_i \dot{T}_i + K_i(T_i - T_{i-1}),$$

where $K_i = \kappa AN/L$ and $c_i = \rho CAL/N$ are the thermal conductance and heat capacity of the $i$th segment, $T_i \equiv T(iL/N,t)$ and

$$\dot{T}_i \equiv [T(iL/N,t + \Delta t) - T(iL/N,t)]/\Delta t.$$

Together with the boundary conditions that

$$T_0(t) = T_0 \text{ (the constant base temperature)},$$

$$T_i(0) = T_0 + P_0 x/KL = T_0 + P_0 i/KN,$$

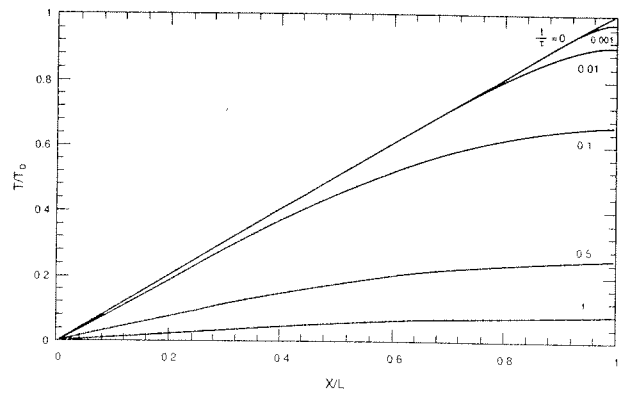


FIG. 3. Model calculations of the temperature distribution along a specimen for seven different values of $t/\tau$. The $t/\tau = 0$ and 0.0001 curves are hardly distinguishable on this scale. The negative curvature of the distribution is the result of temperature decay according to the heat flow equation.

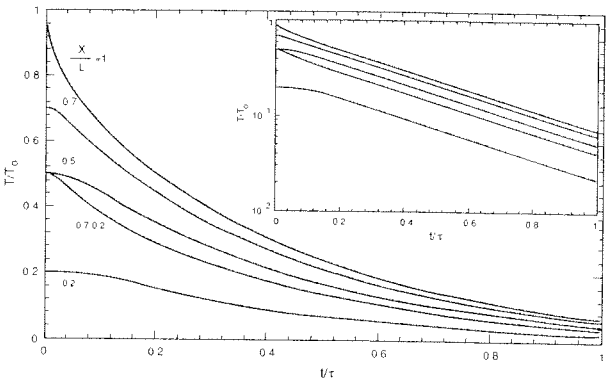


FIG. 4. Temperature of a modeled specimen as a function of time for $x/L = 1$, 0.7, 0.5, and 0.2. Also plotted is $\theta \equiv T(0.7L) - T(0.2L)$. The inset shows the same curves on a logarithmic scale, indicating that $\tau$ is independent of position along the specimen.

and

$$c_N \dot{T}_N + K_N(T_N - T_{N-1}) = 0,$$

the temperature profile of the specimen is computed and plotted in Figs. 3 and 4 as a function of $x/L$ and $t/\tau$. The former shows the temperature profile for seven different values of $t/\tau$ ranging from 0 to 1. Although the $t/\tau = 0$ and 0.0001 curves are hardly distinguishable on the scale used, the temperature at $x = L$ drops instantaneously for any value of $t > 0$. It follows from the heat flow equation that the negative curvature of $T(x,t)$ is a result of the temperature decay. Figure 4 shows the model indeed follows Eq. (4) and the inset shows that the relaxation time is independent of the position along the sample for $t/\tau > 0.1$. Also shown in Fig. 4 is $\theta \equiv T(0.7L) - T(0.2L)$ which is usually about where the thermocouple TC3 is located during the experiment. A plateau at $t \ll \tau$ is present in all $\theta$ curves regardless of the positions, $\Delta t$ or $N$, chosen.

All of these features discussed above are independent of $N$ except the value of $\tau$. Figure 5 shows $\ln[T(L,t)]$ for $N = 2$ to 50. The values of $\tau$ evaluated from the reciprocal of the slope vary from 0.42 for $N = 50$ to 0.64 for $N = 2$. The inset of Fig. 5 shows that $\tau \to 1$ as $N \to 1$, as expected from Eq.(4). Therefore, this model supports the assumption that Eqs.(3) and (4) are valid for our experimental arrangement.

## IV. EXPERIMENTAL TEST

### A. Thermal conductivity

To test our apparatus, we measured $\kappa$ of a GE type 214 fused quartz rod which has a nominal purity of 99.995% by weight of $SiO_2$. Alumina ($Al_2O_3$) is the major impurity, followed by other oxides. The rod measured has a diameter of 2.0 mm and a length of 2.25 cm. The measured $\kappa$ is shown in Fig. 6 as a function of temperature from 4 to 300 K. The solid line represents the TPRC recommended values[8] with about 10% uncertainty. Other reported values vary by as much as an order of magnitude (see, for example, circles[8] in Fig. 6).

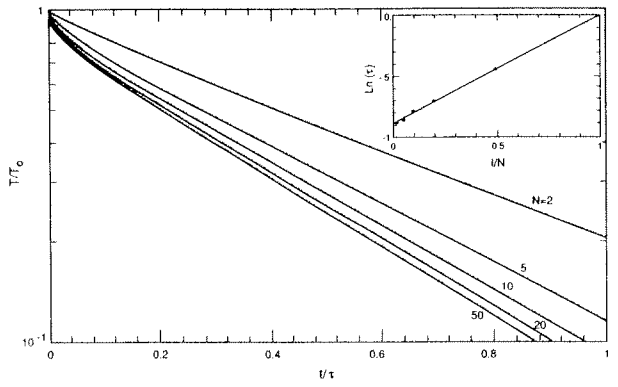


FIG. 5. $T(L,t)$ on a logarithmic scale for different values of $N$. The thermal relaxation times evaluated from these curves are plotted in the inset on a logarithmic scale as a function of $1/N$, showing that $\tau \to 1$ as $N \to 1$.

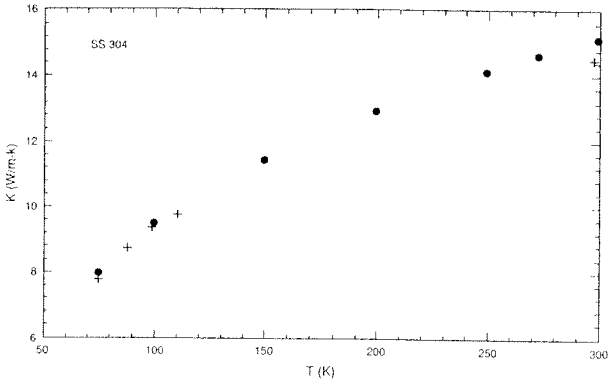


FIG. 7. Measured ( + ) thermal conductivity of a type 304 stainless steel rod compared with the TPRC recommended values (circles) on a linear scale.

The fused quartz is clearly not an ideal material for checking our apparatus because of such a strong sample dependence. In addition, it is necessary to test our experimental setup with electrical conductors as well as insulators. For that we measured $\kappa$ of a AISI type 304 stainless steel rod with dimensions similar to that of the quartz rod. The result is plotted on a linear scale (Fig. 7) together with the TPRC recommended values[9] (circles) with about 5%–10% uncertainty. Our measured $\kappa$ at room temperature is within 4% of the recommended value and is among other reported values which vary as much as by a factor of 2.

## B. Diffusivity and specific heat

The diffusivity of fused quartz has also been measured. Figure 8 shows typical decay curves of $\theta$ for three distinct temperatures, along with $\theta(t)$ from Eq. (4) for $t = 0$–$\tau$. The thermal relaxation times are evaluated from these data and range from a couple of seconds at 4 K to about 6 min. at room temperature. Plotted in the inset are the same curves on a logarithmic scale, showing that they follow Eq. (4) for $t/\tau \geqslant 0.1$. The deviation at $t \simeq 0$ between the three curves shown might be caused by imperfect choices of $\theta_0$ and $\tau$ even though the rest of the curves ($t/\tau > 0.1$) are not as sensitive to such choices. Another possible explanation is that during the temperature cycle, either the small (but finite) thermal resistance of the GE varnish 7031 between the TC and the sample changed, or the position of the TC3 on the sample shifted. No matter which is the dominate effect, it does not seem to cause a significant error in our measurement of $\kappa$ and $C$ as shown. The diffusivity of the fused quartz at room temperature is calculated to be 0.0093 $cm^2/s$, which is in agreement of the manufacturer's data of about 0.009 cm /s.

Using the measured $\kappa$ and $\tau$, the values of $C$ are calculated and shown in Fig. 9 along with that reported by three other groups.[11] The difference between the measured $\kappa$ and the recommended values shown in Fig. 7 is more likely a result of sample dependence and not geometrical factors because such an error would otherwise show up in the $C$ measurement as well.

## V. SOURCE OF ERROR

The uncertainty in the measurement can be divided into geometrical and experimental errors. Geometrical error comes primarily from uncertainty in the positions of TC3 and of the cross-sectional area of the sample. Each of these can introduce a constant error of as much as 10%. Sources of

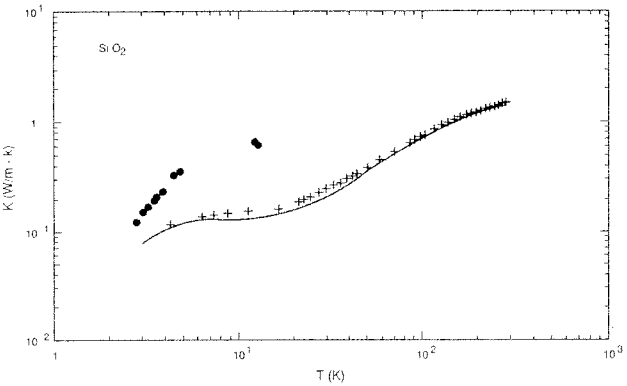


FIG. 6. Measured ( + ) thermal conductivity of a fused quartz rod and the TPRC recommended values (solid line). Also plotted is one of the reported values (circles) from the TPRC Data books.

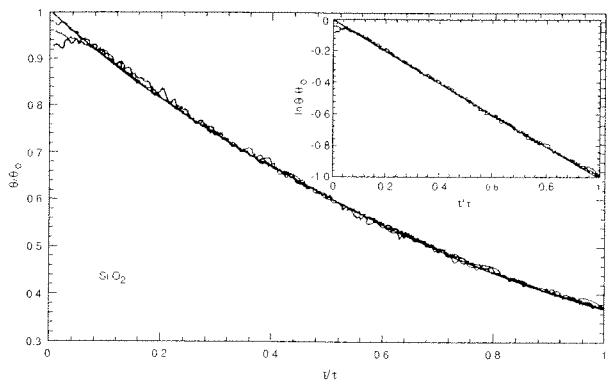


FIG. 8. Typical $\theta$ decay curves for three distinct temperatures plotted along with $\theta(t)$ from Eq. (4). The inset shows the same curves on a logarithmic scale.

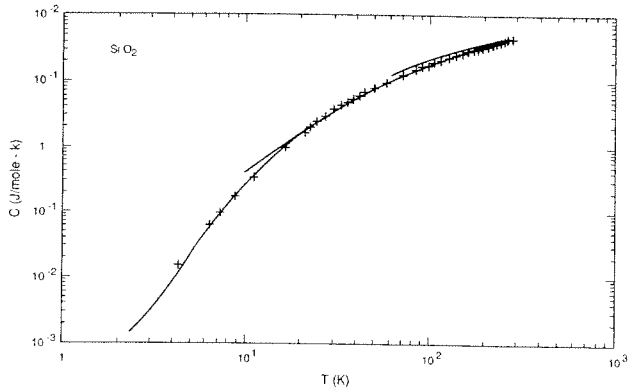


FIG. 9. Specific heat of fused quartz evaluated from the diffusivity measurement ( + ) compared with reported values from three different groups (solid lines).

experimental errors are (1) noise from the nanovoltmeter, (2) thermoelectric voltage pick up through the leads, and (3) determination of $\tau$ from the $\theta$ decay curve. The first one is minimized by taking data for 5–20 min. so that the standard deviation of $\kappa$ is $<0.5\%$. The second one was monitored from time to time throughout the experiment and found to be $<0.5\,\mu$V, which is about 2%–3% of the signal. However, this is not significant for data taken over a limited temperature range and therefore we have a relative resolution of better than 0.5%. This is ideal for study of phase transition at high temperature like the Peierls transition in the charge-density-wave materials.[12] The determination of $\tau$ is estimated to have an uncertainty of $<2\%$, judging from the curves shown in Fig. 8.

## VI. COMMENTS

The advantage of this procedure is that $\kappa$ and $C$ can be determined simultaneously on the very same sample under the same conditions. Although it takes about 2–6 h for each data point on the diffusivity measurement, the fully automated system requires very little attention from the operator. Since the ac amplification techniques are inapplicable, a rather large temperature gradient is used to give an adequate signal-to-noise ratio in the measured dc temperature difference ($\simeq 1$ K at room temperature and $\leqslant 0.5$ K below 50 K), even though this ratio has been improved tremendously by averaging the data for a long period of time. Another disadvantage is that there are geometrical restrictions on the sample to be measured. Also, a bigger sample can be less homogeneous than a smaller single crystal. However, if such a sample is available, the system is capable of measuring $\kappa$ and $C$ simultaneously from room temperature down to liquid helium temperature automatically with an accuracy of better than 3%.

## ACKNOWLEDGMENTS

The authors would like to thank J.D. Thompson and G. Gruner for their useful discussions. We are also indebted to A. Migliori for his assistance. Work at Los Alamos was performed under the auspices of the U.S. Department of Energy. Work at UCLA was supported in part by NSF Grant No. DMR 86-20340.

[1]See, for example, W. D. Seward and V. Narayanamurti, Phys. Rev. **148**, 463 (1966), or J. P. Harrison, Rev. Sci. Instrum. **39**, 145 (1968).
[2]See, for example, G. C. Glatzmaier and W. F. Ramirez, Rev. Sci. Instrum. **56**, 1394 (1985).
[3]See, for example, *Thermal Conductivity*, edited by R. P. Tye (Academic, New York, 1969), Vols. 1 and 2; *Methods of Experimental Physics*, edited by K. Lark-Horovitz and V. A. Johnson (Academic, New York, 1959), Vol. 6A; or *Conduction of Heat in Solids*, edited by H. S. Carslaw and J. C. Jaeger (Clarendon, Oxford, 1959).
[4]R. Bachmann, F. J. DiSalvo, Jr., T. H. Geballe, R. L. Greene, R. E. Howard, C. N. King, H. C. Kirsch, K. N. Lee, R. E. Schwall, H.-U. Thomas, and R. B. Zubeck, Rev. Sci. Instrum. **43**, 205 (1972).
[5]Thermophysical Properties Research Center, Purdue University, IN.
[6]Supplied by Thermalloy, Inc., Dallas, TX.
[7]A. Migliori, Los Alamos National Laboratory LAUR No. ENG-SPTL-33, 1978 (unpublished).
[8]Y. S. Touloukian, R. W. Powell, C. Y. Ho, and P. G. Klemens, Eds., *Thermophysical Properties of Matter*, Vol. 2 of *Thermal Conductivity—nonmetallic solids*, TPRC data series (IFI/Plenum Data Corporation, New York, 1970). Also see references therein.
[9]Y. S. Touloukian, R. W. Powell, C. Y. Ho, and P. G. Klemens, Eds., *Thermophysical Properties of Matter*, Vol. 1 of *Thermal Conductivity—metallic elements and alloys*.
[10]*GE Fused Quartz Products*, General Electric general catalog 7700 (1989).
[11]P. Flubacher, A. J. Leadbetter, J. A. Morrison, and B. P. Stoicheff, J. Phys. Chem. Solids **12**, 53 (1959); R. Wietzel, Z. Anorg. Chem. **116**, 71 (1921); W. Nernst, Ann. Phys. **36**, 395 (1911).
[12]R. S. Kwok and S. E. Brown, Phys. Rev. Lett. **63**, 895 (1989).